

GROWTH, CHARACTERIZATION, NLO AND BIOLOGICAL ACTIVITIES OF Co (II) IONS DOPED Mn (II) L-HISTIDINE HYDROCHLORIDE MONOHYDRATE CRYSTALS

J. Sai Chandra*, V.Parvathi and Dr.Y.Sunandamma

Dept. of Chemistry, Acharya Nagarjuna University, Nagarjuna Nagar-522 510, India.

Article Received on
23 Dec 2014,

Revised on 17 Jan 2015,
Accepted on 11 Feb 2015

*Correspondence for

Author

Dr.Y.Sunandamma

Assistant Professor

Department of Chemistry

Acharya Nagarjuna

University, Nagarjuna

Nagar-522 510, India

ABSTRACT

NLO active and thermally stable Co(II) doped Mn(II)L-Histidine hydrochloride crystals are grown by slow evaporation technique at room temperature from aqueous solutions. The grown crystals are characterized by powder X-Ray diffraction, EPR, FTIR, UV-VIS, ¹H NMR, ¹³C NMR, Mass spectral analysis, Thermal analysis, SEM, Chemical etching and Vicker's micro hardness studies. Both the measured NLO and antibacterial activity of the grown crystals is encouraging.

KEYWORDS: L-Histidine, NLO, Thermal, Morphological and Biological Studies.

1. INTRODUCTION

Crystal growth has taken over as an important interdisciplinary subject covering Physics, Chemistry, Material science, and Chemical engineering, Metallurgy, Crystallography and Mineralogy etc. Growing interest in crystal growth processes is evident from their increasing demand for technological applications.^[1,2] Applications of crystals in semiconductor devices like electrical diodes, photodiodes, transistors, integrated circuits, magnetic devices like tape heads, transformer cores, superconductors, optoelectronics, quantum electronics, nonlinear optics and telecommunications are readily found.^[3-5] Today, the developments in electronics industry, photonics industry, fiber-optic communications and modern optical equipments would not have been possible without perfectly grown crystals.

Amino acids are organic molecules characterized by carboxylic and amino groups with a general formula NH₂-CH(R)-COOH where R is a group characteristic of the molecule.

In the field of NLO crystal growth, amino acids play an important role because crystals capable of generating second harmonics must have a unit cell with no centre of inversion and this requirement is met by amino acids.^[6-8] Optically active amino acids show highly efficient optical second harmonic generation (SHG) properties. Complexes of amino acids too are promising materials for optical second harmonic generation in laser and optical communication technology as they have the advantages of i) derived from organic amino acids and inorganic salts^[9] and ii) crystals are grown below their melting points by solution growth technique.

L-Histidine (L-amino- β -imidazole propionic acid) is characterized among the amino acids by the presence of imidazole ring. It is the only amino acid having an imidazole side chain with pK_a near neutrality. L-Histidine serves as a proton donor, proton acceptor, and nucleophilic agent, occurs frequently at the active sites of enzymes and coordinates ions in larger protein structures.^[10] It is an optically active amino acid and when combined with a suitable inorganic compound, it forms an eccentric crystal with a point group lacking centre of symmetry. A number of L-Histidine complexes were studied for the same reason and recent studies reviewed reveal that L-Histidine family of NLO single crystals are a class of potential materials possessing excellent optical, thermal and mechanical properties for applications in photonic devices.

Doping is the practice of adding impurities to a substance in very low concentrations in order to alter the physical properties of the substance. Great attention has been paid to the study the influence of doping on several crystals because doping can modify the electrical or optical properties of materials for technological applications.^[11-14] Transition metal ions dopants modify crystal morphology and when incorporated into a lattice, play an important role in enhancing the properties of the host materials. Transition metal ion doped crystals with their interesting spectroscopic properties presents themselves as suitable materials for laser and optical fiber applications. Another aspect of doping is it improves the physico-chemical properties of amino acid crystals. Transition metal ion doped amino acids and amino acid complexes are considered as novel, promising materials for second harmonic generation (SHG) properties and are useful as models in understanding the bonding properties of metal ions in metalloproteins.^[15-18]

Cobalt is an essential trace element for all multi cellular organisms, influences various enzymatic functions and is an active center of coenzymes, cobalamins. Cobalt based vitamin

B12 is essential for mammals. Cobalt is also an effective inhibitor of growth and respiration in various microorganisms.^[19] Cobalt(II) ion interactions with various amino acids as mixed ligand complexes were reported in the literature.^[20-27] Triglycine sulfate (TGS) single crystals doped with Co(II) ions were grown from aqueous solution and the effect of dopants on the growth, dielectric, pyroelectric, optical and mechanical properties was investigated.^[28] As far as our literature search goes, only one crystal system, Zinc (D,L-Histidine)₂ complex with Cu(II) ion as dopant was reported.^[29] Other than this particular study, few transition metal ions were reported as dopants on L-Histidine complex crystal systems. Mn(II) L-Histidine complex was chosen as a host lattice because Mn(II) interacts very strongly with L-Histidine to form a stable Mn(II) L-Histidine complex.^[30]

Biological activities of the amino acid complexes or doped amino acid complexes constitute an interesting aspect of study. Generally amino acid complexes are active against gram-positive organisms. High antibacterial activities were exhibited by Leucine and Histidine complexes of Cobalt and Copper towards microorganisms like *Escherichia coli*, known to be multi-resistant to drugs.^[31]

In the present study, we have grown Co(II) ion doped Mn(II) L-Histidine hydrochloride monohydrate complex crystals by slow evaporation technique and characterized them by various spectroscopic techniques like powder X-Ray diffraction, EPR, FT-IR, UV-Vis, NMR and Mass spectral analysis. TG/DTA, DSC, SEM, Microhardness studies, Etching studies and SHG activity by Nd: YAG laser studies were carried out on the grown crystals to ascertain their thermal and mechanical stabilities. Antimicrobial activities of these doped complex crystals were screened for three bacterial species.

2. EXPERIMENTAL DETAILS

Growth of Co(II) ions doped MnLHICl Monohydrate crystal

Mn(II) L-Histidine hydrochloride monohydrate crystals, here after called MnLHICl, were grown by slow evaporation at room temperature from the aqueous, equimolar and equivolume solutions containing Manganese chloride hexahydrate (MnCl₂.6H₂O) [0.1 mol] and L-Histidine hydrochloride monohydrate (C₆H₁₂ClN₃O₃) [0.1 mol]. Co(II) ion doped Mn(II)LHICl crystals were grown by adding 0.01mol % of Co(II) chloride solution to the growth solution. The solution was stirred for 2 h with a magnetic stirrer to obtain a homogeneous mixture and filtered through a Whatman filter paper. The solution was then transferred into a fresh 100 ml beaker and covered with a porous aluminum foil before

leaving it for slow evaporation at room temperature. Violet colored Co(II) ions doped MnLHCl monohydrate crystals with maximum grown dimensions of 15 x 10 x 5 mm³ were obtained in a period of 45- 50 days.

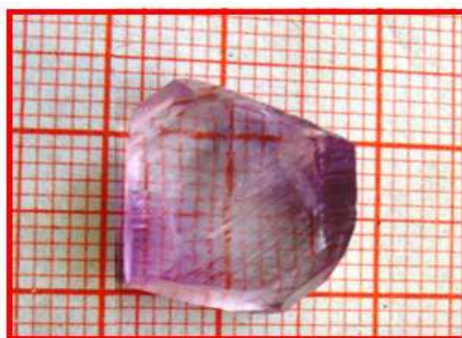


Fig. 1 Co(II) ions doped MnLHCl crystal as grown

Characterization Techniques

XRD spectra were recorded on PHILIPS Make PW1830 X-RAY Diffractometer with $K\alpha$ ($\lambda = 1.54056\text{\AA}$) radiation, EPR spectra were recorded at room temperature on JEOL Make JES-FA 200 EPR Spectrometer, FT-IR spectra were recorded using KBr pellets on Thermo Nicolet 6700 in the range 400- 4000 cm^{-1} , UV-VIS spectra were recorded in the range of 200–1400 nm on JASCO V670 Spectrophotometer, ¹HNMR, ¹³CNMR spectrum were recorded on Bruker AvII-400 MHz, Mass spectra on JEOL SX-102(FAB), TG/DTA analysis on Q500 TA Instruments, DSC curves were recorded using DSC Q20 V24.11, SEM studies by SEM Hitachi- S520, Micro hardness studies by HM-210 Vickers microhardness tester, Chemical Etching studies by Metallurgical microscope (Axioskop 40 MAT), NLO activity by Q switched High energy Nd: YAG Laser- Quanta Ray : Model Lab-170-10 - Energy – 850 mJ /1064 nm and biological activities were carried out by well diffusion method.

3. RESULTS AND DISCUSSION

3.1 Powder X-ray Diffraction Studies

The powder XRD patterns of Co(II) ions doped MnLHCl crystals shown in **Fig.2** revealed sharp patterns indicative of good crystalline phases with a single phase nature. Lattice cell parameters reported from X-Ray patterns of pure (undoped) LHCl^[32] and the lattice cell parameters evaluated for Co(II) ions doped MnLHCl, are shown in **Table1**. The evaluated lattice cell parameters for Co(II) ions doped MnLHCl crystal were $a = 1.5362$, $b = 0.8894$, $c = 0.6873$ nm and $V = 939.06 \text{\AA}^3$. A marginal increase in volume was observed for the Co(II) ion doped MnLHCl crystal compared to pure LHCl, attributed to Co(II) ions inclusion and

weak interactions in the crystal lattice due to low charge on cobalt ion.^[32] The single phase nature of the doped crystal after complexation and doping was also verified with slight shifts in the peak positions in doped LHICl crystals.^[33,34] Slight variations were observed in the unit cell parameters of Co(II) ions doped MnLHICl crystal compared to pure LHICl crystal were interpreted on the same lines i.e., larger amino acid molecules inside interstitial voids and small strain on the lattice due to the presence of metal ions in the host lattice.^[35-37] The *h k l* values along with *d*-spacing's and 2θ , both observed and calculated are shown in **Table 2** for Co(II) ions doped MnLHICl crystals. An orthorhombic system with a space group $P2_12_12_1$ was proposed for Co(II) ions doped MnLHICl crystals with slight changes in the lattice parameters of the crystal due to metal ion inclusions.

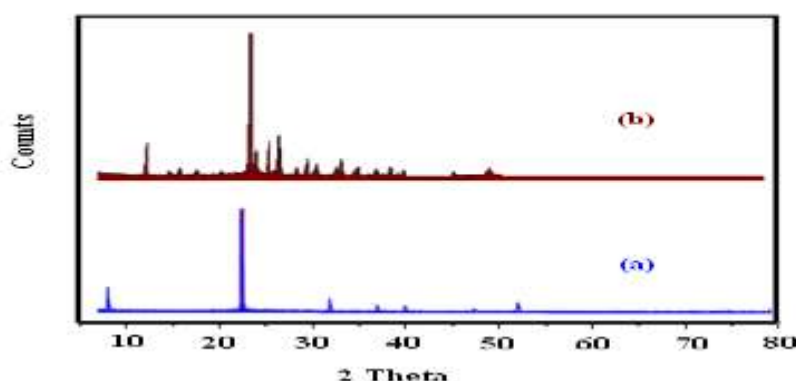


Fig. 2 XRD patterns of (a) LHICl (b) Co(II) ions doped MnLHICl crystals

Table 1: Lattice cell parameters for Pure LHICl and Co(II) ions doped MnLHICl crystals

S.No	Name of compound	Lattice cell parameters (nm)	System	Space group	Volume (Å ³)
1.	Pure LHICl	a = 1.5301 b = 0.8921 c = 0.6846	Orthorhombic	$P2_12_12_1$	934.54
2.	Co(II) ions doped Mn(II)LHICl	a = 1.5362 b = 0.8894 c = 0.6873	Orthorhombic	$P2_12_12_1$	939.06

Table 2 Experimental and calculated XRD data for Co(II) ions doped MnLHICl crystal

d-spacing (Å)	Relative	Indices	2θ (degree)
---------------	----------	---------	--------------------

Obs.	Calc.	Intensity (%)	h	k	l	Obs.	Calc.
7.5036	7.681	10	2	0	0	11.78	11.51
5.7461	5.8132	3.3	2	1	0	15.41	15.23
5.0790	5.1207	2.6	3	0	0	17.45	17.35
3.7922	3.8405	100	4	0	0	23.44	23.14
3.7006	3.7281	11	3	1	1	24.03	23.85
3.4988	3.5258	15	4	1	0	25.44	25.24
3.4060	3.4365	2.5	0	0	2	26.14	25.91
2.8852	2.904	5.1	1	0	5	30.97	30.76
2.5488	2.5603	2.6	6	0	0	35.18	35.02
2.3963	2.3993	2.8	6	0	1	37.50	37.45
1.9891	2.0005	0.7	6	1	2	45.57	45.59
1.9048	1.8924	4.2	3	2	3	47.79	48.84

3.2 EPR Spectral Studies

Electron Paramagnetic Resonance (EPR) is an extremely important technique for identifying the site symmetry and the defects in doped crystals.

Co(II) is a d^7 ion and in an octahedral symmetry d^7 configuration has an orbital triplet state. The lowest triplet state is split due to spin-orbit coupling and gives a ground state Kramer's doublet. The next excited states differ by a few hundred wave numbers higher in energy. Distortions, which lower the symmetry, mix these states. Therefore, the g values become anisotropic and are sensitive to variations in the crystal field.^[38] EPR spectrum of Co(II), in general, is observed only at low temperature because the spin lattice relaxation time is extremely short for Co(II) ions in octahedral coordination. At higher temperatures, the spectrum becomes broader, probably due to short relaxation time, characteristic of high spin state of Co(II) ions.^[39-41] Mn(II) ion exhibits well resolved EPR spectra due to long spin-lattice relaxation times in the ground state at room temperature. For Mn(II) ion, the ground state is $^6S_{5/2}$, exhibits a split due to spin-spin interaction resulting in three Kramer doublets with separations of $4D$ and $2D$. These doublets split further by the application of external magnetic field into six levels with successive separations of $g\beta B + 4D$, $g\beta B + 2D$, $g\beta B$, $g\beta B - 2D$ and $g\beta B - 4D$. The transitions between these levels give rise to five equally spaced lines, each of which further splits into a sextet due to hyperfine interaction from the nuclear spin of $^{55}\text{Mn}(I = 5/2)$. Hence one can observe a 30 line pattern per molecule per unit cell^[42] in the crystal lattice for Mn(II) ion in the host lattice.

Fig. 3 shows the EPR spectrum of Co(II) ion doped MnLHICl at room temperature. Basic and standard patterns were observed for Mn(II) ion in the host lattice of the EPR spectrum of

Co(II) ions doped MnLHCl crystal. Two resonance signals observed in the spectrum corresponding to g values, $g = 2.0308$ and $g = 4.3242$ were characteristic of Co(II) ions, while the resonance line at $g = 2.0308$ might have resulted due to overlap of spin-lattice relaxations of Mn(II) and Co(II) ions in the host lattice. Thus $g = 4.32$ resonance line was attributed to Co(II) ions in octahedral symmetry and the $g = 2.03$ line was also an indication of random distribution of distortions.^[43-46] Broadness of resonance peaks characteristic of Co(II) ions were found to increase in the spectrum at room temperature. The line broadening was interpreted in terms of dipolar interactions of paramagnetic host lattice with the paramagnetic dopant ion. From EPR studies, we concluded that Co(II) ions were distributed in the host lattice in an octahedral symmetry, slightly distorted.

By correlating EPR and optical absorption spectral data, the covalency parameter (k_o) was evaluated by the following relation^[47]

$$g = 3.33 + k_o - 7.5(\lambda/\Delta)$$

where g is the observed g -factor, λ is the spin – orbit coupling constant and Δ is the energy difference between ${}^4T_{1g}(F) \rightarrow {}^4T_{2g}(F)$.

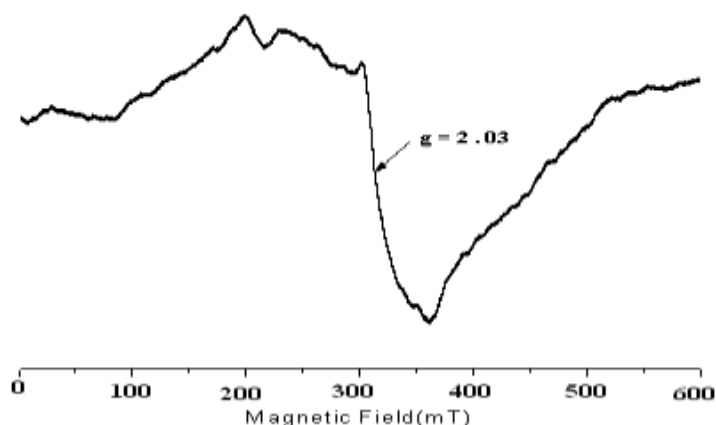


Fig. 3 Polycrystalline EPR spectrum of Co(II) doped MnLHCl crystal. ($\nu = 9.156889$ GHz)

The k_o value lies between 0.5 and 1.0, the limits of pure covalent and pure ionic bonding respectively. The calculated k_o value of 1.0 indicated that the bonding between the Co(II) ions and the ligands was moderately covalent in nature.

3.3 FT-IR Spectral Studies

FTIR analysis is important for the identification of the presence of various functional groups in the grown crystals. FTIR spectrum of Co(II) ions doped MnLHICl crystals is shown in **Fig. 4**. IR spectral bands of Co (II) doped MnLHICl crystals were interpreted and compared with the known spectrum of pure(undoped) LHICl.^[48] FTIR spectrum of Co(II) ions doped MnLHICl showed a strong and intense peak at 3405 cm^{-1} and was assigned to O–H stretching of carboxylic acid/ presence of water molecule in the crystal. Peak at 3076 cm^{-1} assigned to NH in amine functional group and peak at 2987 cm^{-1} assigned to NH_3^+ stretching were recorded in the spectrum. Presence of aromatic and aliphatic C–H stretching vibrations at 2890 and 2611 cm^{-1} respectively and a strong and broad peak at 1605 cm^{-1} due to C=O group was recorded in the spectrum. Asymmetric and symmetric bending vibrations for NH_3^+ at 1574 and 1411 cm^{-1} respectively and asymmetric and symmetric stretchings of COO^- were recorded at 1492 and 1331 cm^{-1} respectively in the spectrum. Strong peaks at 1133 and 1061 cm^{-1} were attributed to aromatic C–N and C–O stretching vibrations of carbonyl group respectively. A broad band from 3200 to 2100 cm^{-1} assigned to asymmetric and symmetric stretching vibrations of O–H, N–H, and 956 , 863 and 621 cm^{-1} for C–H and ring asymmetric and symmetric stretchings and ring deformation respectively in the doped crystal.

Significant shifts were observed in the characteristic vibrational frequencies in the FT-IR spectrum of Co(II) ions doped MnLHICl monohydrate crystal compared to undoped LHICl. These shifts were attributed to changes in the nature of bonding due to complexation and doping in the crystal. Coordination of LHICl to Mn(II) ion as a tridentate ligand was evident from the shifts in the frequencies of coordinating groups. Shifts in the resonance frequencies from 3157 cm^{-1} in LHICl to 3076 cm^{-1} in the doped complex for amine nitrogen, from 1143 to 1133 cm^{-1} for imidazole nitrogen and from 1637 to 1605 cm^{-1} for carboxyl oxygen were observed supporting the tridentate nature of L-Histidine in coordination with Mn(II) ion. A strong bonding between the ligand and the metal ion Mn(II) was observed in the Co(II) doped complex compared to other transition metal ion doped LHICl complexes synthesized in our laboratory. All the other frequencies characteristic of amino acid complexes were observed in the FTIR spectrum of the doped complex. Shifts observed in the frequencies of all the other groups was an indication that the Co(II) ions doped MnLHICl complex crystal had its own structure which differed in bond characters from pure LHICl. The reported and observed IR frequencies are summarized in **Table 3**.

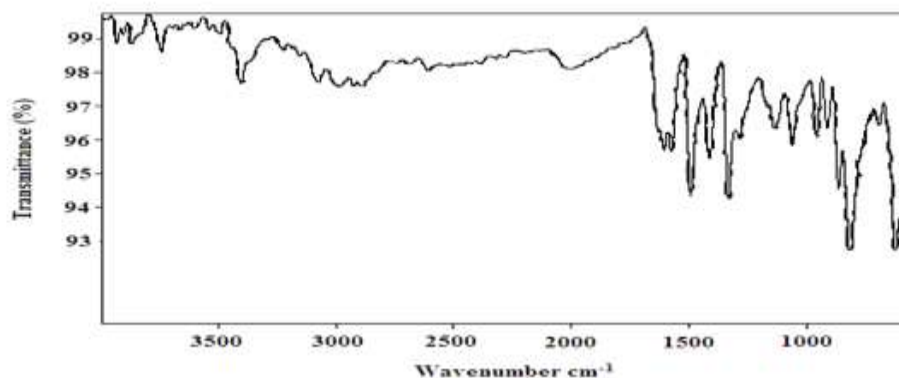


Fig. 4 FTIR spectrum of Co(II) doped MnLHCl crystal

Table 3 Observed vibrational modes of LHCl and Co(II) doped MnLHCl crystals

Pure LHCl (cm ⁻¹)	Co(II) ions doped Mn LHCl (cm ⁻¹)	Assignments
3411	3405	O-H Stretching water
3157	3076	N-H stretching
3106	2987	NH ₃ ⁺ stretching
3019	2890	Aromatic C-H Stretching
2712	2611	Aliphatic C-H Stretching
2009	2004	Overtone and combination modes
1637	1605	C=O stretching
1606	1574	Asymmetric bending of NH ₃ ⁺
1580	1492	Asymmetric stretching of COO ⁻
1497	1411	Symmetric bending of NH ₃ ⁺
1414	1331	Symmetric stretching of COO ⁻
1143	1133	C-N stretching
1064	1061	C-O Stretching of carbonyl group
959	956	Ring asymmetric stretching
867	863	Ring symmetric stretching
834	813	O-H Stretching water
630	621	Ring deformation

3.4 UV-VIS Spectral Studies

Co(II) is a d⁷ ion and in a high spin state it gives rise to free ion terms ⁴F, ⁴P, ²G and several other doublet terms. In a weak octahedral crystal field, the term ⁴F splits into ⁴T_{1g}(F) + ⁴T_{2g}(F) + ⁴A_{2g}(F), the term ²G splits into ²A_{1g}(G) + ²T_{1g}(G) + ²T_{2g}(G) + ²E_g(G) and ⁴P term transforms as ⁴T_{1g}(P). The term ⁴T_{1g}(F) occupies the ground state in octahedral crystal field. In strong crystal fields (Dq >1500 cm⁻¹), the term ²E_g(G) is the ground state and in intermediate crystal fields (Dq ≈ 850cm⁻¹), the term ⁴T_{1g}(G) is the ground state. In general for Co(II) with d⁷ configuration in the octahedral field, without spin-orbit interaction three spin allowed transitions ⁴T_{1g}(F) → ⁴T_{2g}(F), ⁴T_{1g}(F) → ⁴A_{2g}(F) and ⁴T_{1g}(F) → ⁴T_{1g}(P) are possible. Of these three transitions, ⁴T_{1g}(F) → ⁴A_{2g}(F) transition is a weak transition.^[49]

The optical absorption spectrum recorded for Co(II) ions doped MnLHCl crystals in the wavelength range 200–1400 nm is shown in Fig. 5. The bands obtained at 375, 420 and 545 nm were assigned to Mn(II) ion corresponding to the transitions ${}^6A_{1g}(S) \rightarrow {}^4T_{2g}(G)$, ${}^6A_{1g}(S) \rightarrow {}^4A_1(G)$ and ${}^6A_{1g}(S) \rightarrow {}^4T_{1g}(G)$ respectively. Crystal field splitting parameter (Dq) and the inter-electron repulsion (Racah) parameters B and C with the Trees correction factor, α were calculated for Mn(II) ion as $Dq = 750$, $B = 755$, $C = 2920 \text{ cm}^{-1}$ and $[\alpha] = 76 \text{ cm}^{-1}$ and the values were found to be in good agreement with those reported in the literature.^[50] The values are presented in Table 4.

UV-VIS absorption studies recorded three characteristic bands, two of them intense at 595 and 1195 nm assigned to spin allowed ${}^4T_{1g}(F) \rightarrow {}^4T_{1g}(P)$ and ${}^4T_{1g}(F) \rightarrow {}^4T_{2g}(F)$ transitions respectively and a weak band at 1096 nm due to spin forbidden ${}^4T_{1g}(F) \rightarrow {}^2E_g(G)$ transition for Co(II) ions. Evaluated values for Co(II) ions for Dq , B , C were $Dq = 940$, $B = 925$ and $C = 3885 \text{ cm}^{-1}$. The analysis of the optical absorption spectrum confirmed the tetragonally distorted octahedral coordination for Co(II) ions in the host lattice.^[51]

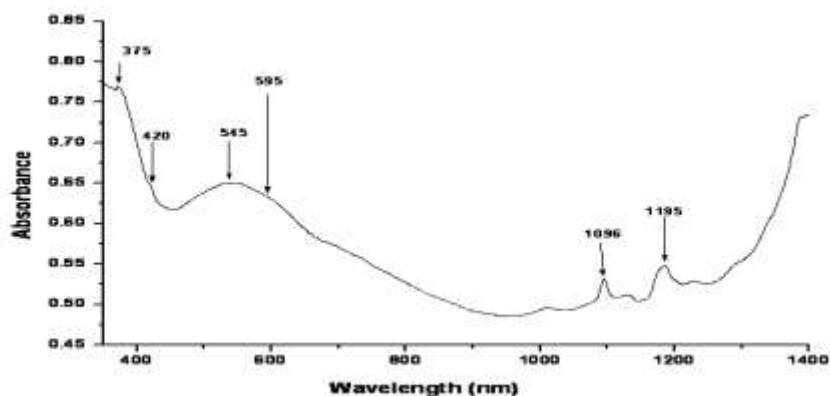


Fig. 5: Optical spectrum of Co(II) ions doped MnLHCl crystal

Table 4: Optical absorption data of Co(II) ions doped MnLHCl crystal

Transition	Wavelength(nm)	Wavenumber (cm^{-1})	
		Obs.	Cal
For Co(II) ions			
${}^4T_{1g}(F) \rightarrow {}^4T_{1g}(P)$	595	16802	16917
${}^4T_{1g}(F) \rightarrow {}^2E_g(G)$	1096	9121	8993
${}^4T_{1g}(F) \rightarrow {}^4T_{2g}(F)$	1195	8365	8219
$Dq = 940$, $B = 925$, $C = 3885 \text{ cm}^{-1}$			
For Mn(II) ion			
${}^6A_{1g}(S) \rightarrow {}^4T_{2g}(G)$	375	26659	26335
${}^6A_{1g}(S) \rightarrow {}^4A_1(G)$	420	23803	23670
${}^6A_{1g}(S) \rightarrow {}^4T_1(G)$	545	18343	17647
$Dq = 750$, $B = 755$, $C = 2920 \text{ cm}^{-1}$, $[\alpha] = 76 \text{ cm}^{-1}$			

3.5 ^1H NMR Spectral Studies

The ^1H NMR spectrum of Co(II) ions doped MnLHCl crystal is shown in **Fig. 6** and the values for LHCl and Co(II) doped MnLHCl are shown in **Table 5**. Compared to the reported resonances for pure LHCl for H_α , H_β , and H-2 and H-4 of imidazole ring,^[52] the ^1H NMR spectrum of Co(II) doped MnLHCl crystal exhibited H_α resonance as a triplet centred at 3.96 ppm, H_β resonance around 3.28 ppm and H-2 and H-4 of imidazole ring at 8.60 and 7.33 ppm respectively. Both the H_α and H_β resonances moved upfield in the complex compared to pure LHCl due to complex formation/deprotonation of the carboxylic group.^[53] The two resonances for H-2 and H-4 of imidazole ring were also found to move upfield in the doped complex indicating a change in the environment due to complex formation and doping.

Table 5: Resonance peaks in ^1H NMR for LHCl and Co(II) ions doped MnLHCl crystals

Spectrum	Signals of δ (ppm)		Resonances
	Pure LHCl	Co(II) ions doped MnLHCl	
^1H NMR	4.35	3.98,3.96,3.95	H_α
	3.47	3.29,3.27	H_β
	8.73	8.60	H-2 of imidazole ring
	7.48	7.33	H-4 of imidazole ring

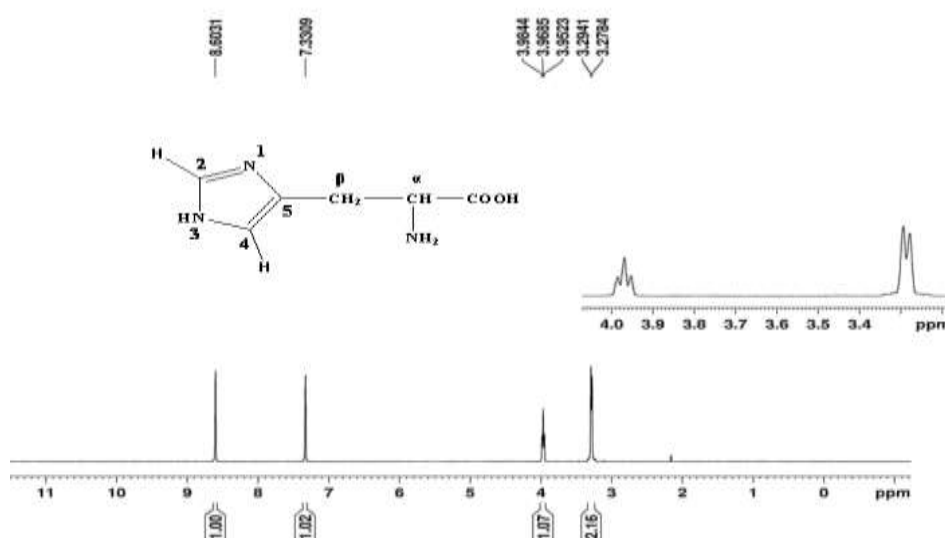


Fig. 6: ^1H NMR Spectrum of Co(II) doped MnLHCl crystal

3.6 ^{13}C NMR Spectral Studies

Carbon atoms present in various chemical environments and thus the functional groups present in the compounds could be identified by ^{13}C NMR spectral study. Reported ^{13}C NMR spectrum of LHICI showed six resonance peaks.^[54] The chemical shifts in ^{13}C NMR spectra of LHICI and Co(II) doped MnLHICI crystals are shown in **Table 6**.

Co(II) doped MnLHICI crystal in **Fig. 7** also showed six resonance peaks. The resonance peak resolved at $\delta = 172.34$ ppm was due to the presence of CO group of side chain of L-Histidine. Two consecutive signals resolved at $\delta = 133.95$ and 127.33 ppm were due to the presence of CH groups of imidazole ring. The peak at 117.67 ppm was due the presence of C atoms of the ring. The resonance peaks resolved at $\delta = 53.60$ and 25.85 ppm were due to the presence of CH and CH_2 groups respectively on the side chain of L-histidine in Co(II) doped Mn LHICI crystal. In the spectrum of Co(II) doped MnLHICI crystal, the positions of resonance peaks were slightly shifted from pure LHICI crystal, attributed to the presence of dopant in the crystal.^[55]

Table 6: Chemical shifts in ^{13}C NMR for LHICI and Co(II) doped MnLHICI crystal

Spectrum	Signals of $\delta(\text{ppm})$		Groups
	LHICI	Co(II) ions doped MnLHICI	
^{13}C NMR	176.86	172.34	CO of side chain
	139.20,135.21	133.95,127.33	CH of imidazole ring
	119.23	117.67	C of imidazole ring
	54.43	53.60	CH of side chain
	27.14	25.85	CH_2 of side chain

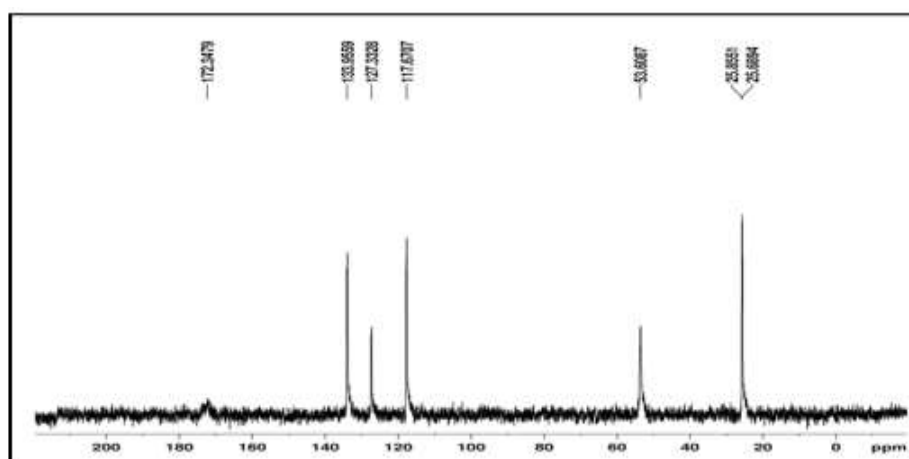


Fig. 7: ^{13}C NMR spectrum of Co(II) doped MnLHICI crystal

3.7 Mass Spectral Studies

The electronic impact mass spectrum of Co(II) ions doped MnLHCl is shown in **Fig. 8**. The spectrum recorded a molecular ion (M^+) peak at $m/z = 305.1$ amu corresponding to major species $[C_6H_{10}Cl_2N_3O_3Mn]^+$ (298.02) with a provision for the inclusion of the doped species, present in low concentrations. The small variation in the molecular weight could also be an indication that the molecular structure included an impurity in the form of a dopant ion. It also showed a series of peaks at 156, 181, 203 and 256 amu corresponding to various fragments of the molecule whose intensities gave an idea of stabilities of the respective fragments.

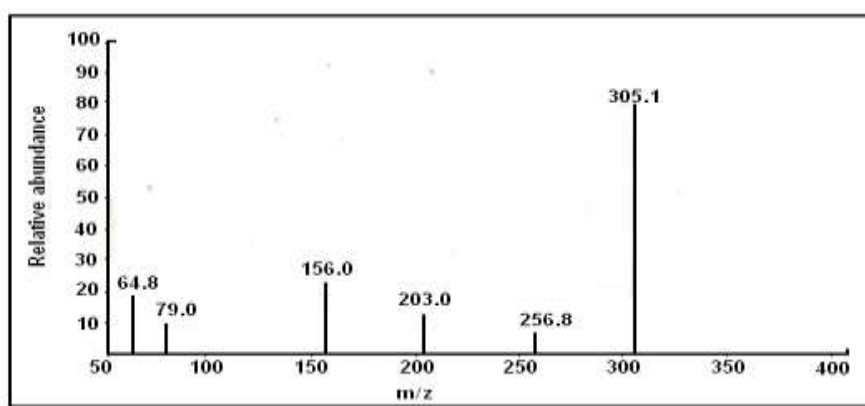


Fig. 8: Mass spectrum of Co(II) doped MnLHCl crystal

3.8 Thermal Studies

TG/DTA and DSC Studies

TG/DTA and DSC studies give ideas about phase transition temperatures and the melting points of the grown crystals and are of immense importance in fabrication technology as they provide information about the thermal stability of the material for fabrication.^[76] Reported studies on TG/DTA and DSC curves of pure LHCl^[20] formed the basis for the interpretation of the results. The simultaneously recorded TG/DTA curves of Co(II) doped MnLHCl are shown in **Fig. 9(a)** and DSC curves in **Fig. 9(b)** TG curve for Co(II) ions doped MnLHCl crystals was smooth with no weight change up to a temperature of 160°C. The first weight loss of 5.12% observed in the temperature range 160 to 201 °C was attributed to the loss of water molecules. A major weight loss was observed in the temperature range 288 – 375 °C due to decomposition and volatilization of the compound. DTA curves for the crystals recorded three endothermic peaks, a sharp peak at 201 °C and two slightly broader peaks at 288 and 375 °C, attributed to loss of crystal water, melting point of the doped crystal and a major weight loss respectively. DSC analysis for Co(II) ions doped MnLHCl crystal

confirmed the same results observed in TG/DTA. The DSC trace was smooth up to 157 °C and two sharp endothermic peaks at 200 and 288 °C were attributed to loss of lattice water and melting point of the compound. Enhanced thermal stabilities for the doped crystals were observed due to inclusion of metal ions compared to uncomplexed and undoped LHIcI.

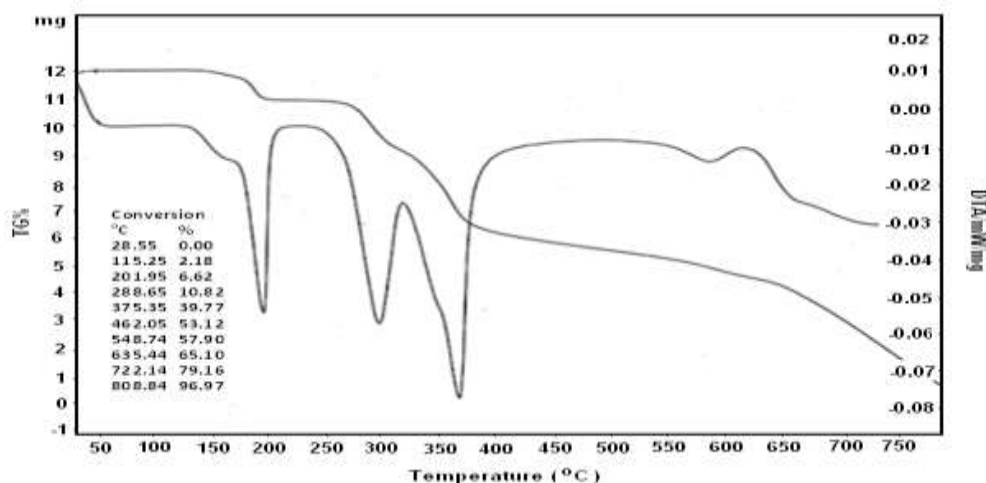


Fig. 9(a) TG/DTA spectrum of Co(II) doped MnLHICl crystal

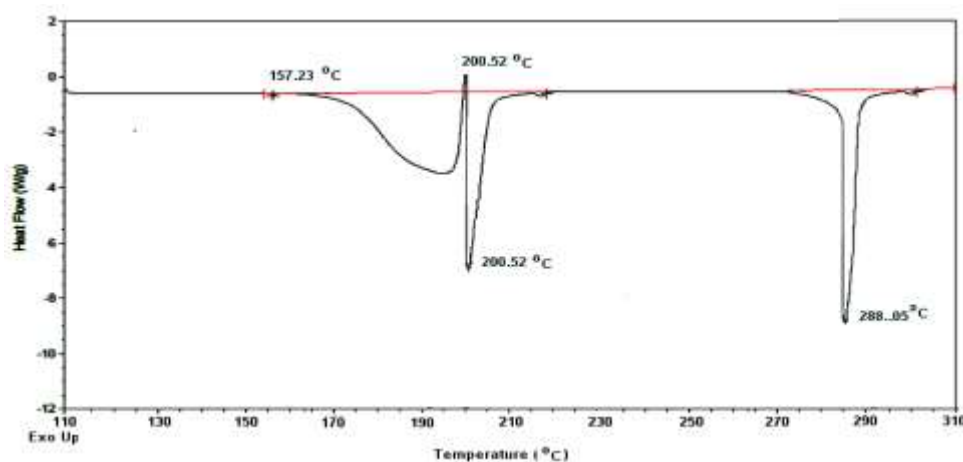


Fig. 9(b) DSC spectrum of Co(II) doped MnLHICl crystal

3.9 SEM and EDAX Analysis

SEM analysis was carried out on the grown crystals to study the nature and surface morphology of the crystals. SEM image of pure LHIcI in **Fig. 10(a(i))** showed a smooth and continuous surface, free from any inclusions, a sign of purity of the compound.^[56] SEM image of Co(II) ions doped MnLHICl shown in **Fig. 10(a(ii))** indicated uneven rough surface and the presence of smaller crystallites could be seen which was attributed to the presence of dopant in the crystalline matrix and temperature fluctuations during the growth process. The greater particle size in general observed for the doped complex crystals was explained by the fact that minimum crystal defects were formed when ions occupy regular lattice sites.^[37]

In order to confirm the presence of elements in Co(II) doped MnLHCl crystals, the sample of grown crystal was subjected to Energy Dispersive X-ray analysis. **Fig. 10(b)** shows the EDAX result of Co(II) ions doped MnLHCl crystals. Identified elements confirmed the presence of Mn and Co in the host lattice.

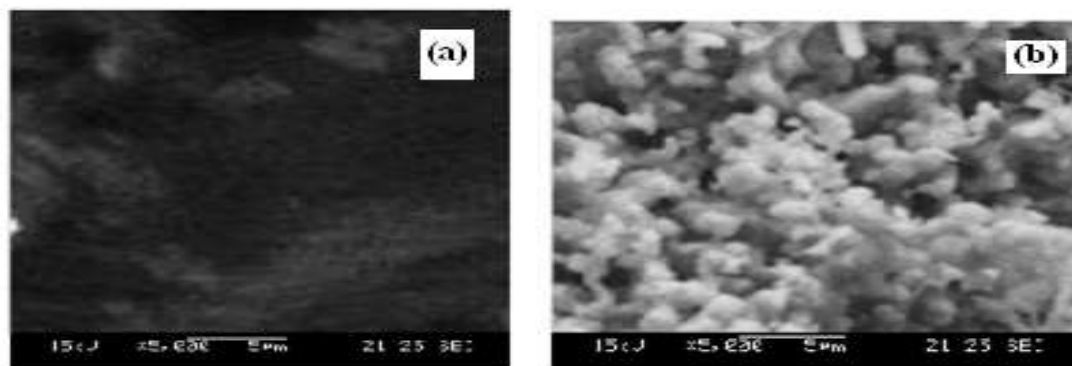


Fig. 10(a) SEM images of (i) Pure LHCl (ii) Co (II) doped MnLHCl crystals

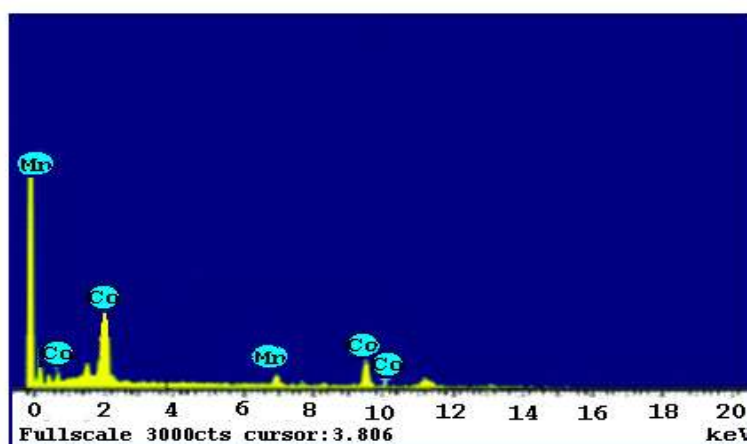


Fig. 10(b) EDAX spectrum of Co(II) ions doped MnLHCl crystal

3.10 Microhardness Studies

Hardness of the material is a measure of resistance offered to deformation. A transparent and polished crystal free from cracks was selected for hardness measurements. The indentations were made on the flat surface with a load ranging from 25 to 100 g. The indentation time was kept as 5s for all the loads. The Vicker's hardness (H_v) was calculated from the relation.^[57]

$$H_v = \frac{1.8544 P}{d^2} \text{ kg/mm}^2$$

Where P is the applied load and d the average length of the diagonal of indentation mark. It was observed that the hardness value increased up to, $H_v = 83.2 \text{ kg/mm}^2$ with an applied

load, $P = 90$ g, due to work hardening of the surface layer. Above 90 g load cracks were formed due to the release of internal stress generated locally by indentation decreasing the hardness value.^[58] The variation of microhardness with applied load for the Co(II) ions doped MnLHCl crystal is shown in **Fig. 11**.

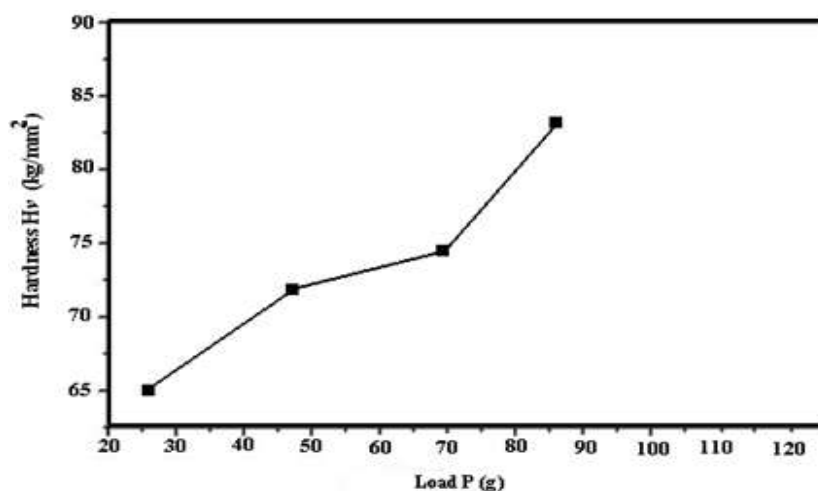


Fig. 11 Microhardness studies of Co(II) ions doped MnLHCl crystal

3.11 Chemical Etching Studies

Etching studies were carried out on the Co(II) ions doped MnLHCl grown crystals in order to study the symmetry of the crystal face from the shape of etch pit and the distribution of structural defects in the grown crystals/ dislocations in the crystal. In the present work water was used as an etchant. A photograph was taken with a maximum etching time of 5s and is presented in **Fig. 12**. It was observed that the deformation of the crystal was minimum in the process of etching with increased time from 10s compared to the pure LHCl crystal.^[37]

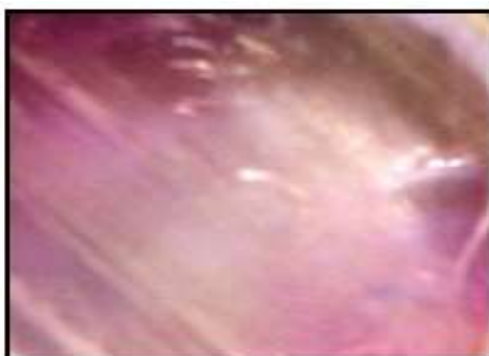


Fig. 12 Etching studies of Co(II) doped MnLHCl crystal

3.12 Nonlinear Optical Activity of Co(II) doped MnLHCl crystal

The Non linear optical activity of Co(II) ions doped MnLHCl was confirmed by Kurtz and Perry powder technique.^[59] The powdered crystal was exposed to a Q-switched Nd: YAG laser beam of wavelength 1064 nm with input energy of 8.8mJ, pulse duration of 8ns, a repetition of 10 Hz and a spot size of 1 mm diameter was used in this technique. The grown crystals were grounded into fine microcrystalline powder and were densely packed between transparent glass slides. Microcrystalline sample of KDP was used for the comparison of conversion efficiencies of the grown crystals. The activity was confirmed by the emission of green radiation of input wavelength 1048nm collected by a monochromator after separating the 1064nm with input power 0.77J pump beam. The SHG efficiency of Co(II) doped Mn(II) LHCl crystal was found to be 7.7 mJ, higher than that of many organic NLO crystals but lower than KDP value (8.8 mJ).

3.13 Biological activity Co(II) doped MnLHCl crystals

The antibacterial activity of the doped complex was tested for Gram positive (*Staphylococcus aureus*, *Streptococcus pneumoniae*) and Gram negative (*Pseudomonas aeruginosa*) bacteria by well diffusion method^[60] shown in **Fig. 13**. Nutrient agar medium was prepared by using peptone, beef extract, NaCl, agar-agar, and distilled water. Twenty five millilitre nutrient Agar media (NA) was poured in each Petri plates. After solidification, 0.1mL of test bacteria spread over the medium using a spreader and were placed at four equidistant places at a distance of 2 cm from the center in the inoculated Petri plates. All determinations were made in duplicate for each compound. An average of two independent readings for each compound were recorded. These Petriplates were kept in refrigerator for 24 hours for prediffusion. Finally, Petri plates were incubated for 26–30 hours $28 \pm 2^\circ\text{C}$.

The biological screening was effective and the results showed a significant antibacterial activity for the Co(II) ions doped MnLHCl (Fig 3.15) crystals over both types of bacterial strains. The inhibition zone diameters in the well diffusion assays are given in **Table 7**. Among the three species, *Staphylococcus aureus* was more sensitive to Co(II) ions doped MnLHCl crystal action. The Sensitivity for three bacterial species follow the order as *Staphylococcus aureus* > *Streptococcus pneumoniae* > *Pseudomonas aeruginosa*.



Staphylococcus aureus Streptococcus pneumoniae Pseudomonas aeruginosa

Fig. 13 Antibacterial activity of Co(II) doped MnLHCl crystal

Table 7 Antibacterial activity of Co(II) doped Mn LHCl crystal

Bacterial strains	Zone of inhibition (mm)*	MIC** (mg/mL)
Staphylococcus aureus	14	500
Streptococcus pneumoniae	12	500
Pseudomonas aeruginosa	11	375

* Used disk with 600 mg of Co(II) ions doped MnLHCl . Number of assays = 3, estimated error \pm 1mm.
 * MIC is the minimum drug concentration required to inhibit bacterial growth. Number of assays = 3

4. CONCLUSIONS

- Violet colored Co(II) doped MnLHCl monohydrate crystals with maximum dimensions $15 \times 10 \times 5 \text{ mm}^3$ were grown and characterized.
- Powder XRD patterns of Co(II) ions doped MnLHCl crystals exhibited crystalline nature, orthorhombic system with space group $P2_12_12_1$ and a marginal increase in volume indicating weak interactions in the doped complex crystal.
- EPR studies concluded that the doped Co(II) ions were distributed in the host lattice in an octahedral symmetry with slight distortion and moderate covalency.
- A strong bonding between the ligand and the metal ion Mn(II) was present as proved by shifts in IR frequencies of the bonding sites in the doped crystals.
- From UV-Vis studies, characteristic metal ion absorptions and crystal field splitting parameter (Dq), inter-electron repulsion (Racah) parameters B and C suggested reduced repulsions due to complex formation in the host lattice.
- Upfield shifts in ^1H NMR and ^{13}C NMR spectra indicated changes in the nature of hydrogen resonances and carbon atom environments respectively due to complex formation and doping.

- Mass spectrum showed molecular ion (M^+) peak at $m/z = 305.1$ amu for a major species $[C_6H_{10}Cl_2N_3O_3Mn]^+$ (298.02) with a provision for the dopant ion inclusion.
- TG/DTA, DSC studies indicated the melting point of the crystal as 288°C , greater than pure LHCl.
- SEM studies showed the presence of smaller crystallites on the surface due to dopant ion and EDAX analysis confirmed the presence of metal ions in the crystal lattice.
- Crystals are mechanically stable with minimum deformations.
- SHG activity was 6.5 mJ.
- The anti bacterial activity of the crystal indicated that *Staphylococcus aureus* was more sensitive to Co(II) doped MnLHCl crystal action.

5. ACKNOWLEDGEMENTS

Authors Y. Sunandamma, J. Sai Chandra and V. Parvathi are thankful to UGC, New Delhi, for financial assistance through UGC-MRP/ F.No. 37-7/2009(SR), J. Sai Chandra particularly thankful to UGC, New Delhi, for financial assistance through Non-SAP meritorious fellowship/Ref. No. F.4-1/2006(BSR).

6. REFERENCES

1. J.C. Brice; Crystal Growth Processes, Halsted Press, John Wiley and sons, Inc., New York., 1986.
2. H.S. Nalwa and S. Miyata; Nonlinear optics of organic molecules and polymers, Eds., CRC Press, Boca Raton, FL., 1997.
3. M.D. Aggarwal and J. Stephens; J. Opto.Adv. Mater., 2003; 5: 3.
4. C. Razzetti, M. Ardoino and C. Paorici; Cryst. Res. Tech., 2002; 37: 456.
5. B.J. McArdle, J. N Sherwood and A. C Damask; J. Cryst. Growth., 1974; 22: 193.
6. C.C. Frazier, M.P. Cockerham, E.A. Chauchard and C. H. Lee; J. Optical Society of America., 1987; 4: 1899.
7. P. Gunter, Ch. Bosshard and K. Sutter; Appl.Phy. Lett., 1987; 50: 486.
8. D. Eimerl, S. Velsko, L. Davis, F. Wang, G. Loiacono and G. Kennedy; IEEE J. Quant. Elec., 1989; 25: 179.
9. M.N. Bhat and S.M. Dharma Prakash; J. Cryst. Growth., 2002; 235: 511.
10. A. Mostad, K.A. Nystol, Chr. Romming and S. Natarajan; Z. Kristallogr., 1995; 210: 352.
11. X. Lai, K.J. Roberts, L.H. Avanci, L.P. Cardoso and J.M. Sasaki; J. Appl. Crystallogr., 2003; 36: 1230.

12. D.A.H. Cunningham, R.B Hammond, X. Lai and K.J. Roberts; *Chem. Mater.*, 1995; 7: 1690.
13. X. Lai, K.J. Roberts, J.M. Bedzyk, P.F. Lyman, L.P. Cardoso and J.M. Sasaki; *Chem. Mater.*, 2005; 17: 4053.
14. C.M.R. Remedios, W. Paraguassu, P.T.C. Freire, J. Mendes-Filho, J.M. Sasaki and F.E.A. Melo; *Phys. Rev. B.*, 2005; 72: 014121.
15. P. C. Thomas, S. Aruna, J. Madhavan, Reena Ittyachan, Joseph Arul Pragasam, Joe. G. M. Jesudurai, K. Prabha and P. Sagayaraj; *Ind. J. Pure and Appl. Phy.*, 2007; 45: 591.
16. Donato Attanasio, Ines Collamati and Claude Daul; *Inorg. Chem.*, 1985; 24: 2746.
17. E. Natarajan and P. Natarajan; *Inorg. Chem.*, 1992; 31: 1215.
18. Robert J. Deeth, Melinda J. Duer, and Malcolm Gerloch; *Inorg. Chem.*, 1987; 26: 2573.
19. D. Burk. J. Hearon, L. Caroline and A. L.Schade; *J.Biol.Chem.*, 1946; 165: 723.
20. P. J. Morris and R. B. Martin; *J. Am. Chem. Soc.*, 1970; 92: 1543.
21. Clifford J. Hawkins and Jill Martin., *Inorg. Chem.*, 1983; 22: 3879.
22. Marianne G. Patch, Kenneth P. Simolo, and Carl J. Carrano; *Inorg. Chem.*, 1982; 21: 2912.
23. S.K. Joshi, V. K Hinge, B. D Shrivastava; *AIP Conf. Proc.*, 2007; 882: 337.
24. Roy. G. Neville; *J. Am. Chem. Soc.*, 1957; 79: 518.
25. D. Boruah; *Int. J. Sci. Res. Pub.*, 2012; 2: 1.
26. M. M. Alam, S. M. M. Rahman, M. M. Rahman and S. M. S. Islam; *J. Sci. Res.*, 2010; 2: 91.
27. T. Varadinova, S. Shishkov, M. Panteva and P. Bontchev; *Met. Based Drugs.*, 1996; 3: 149.
28. Jiann-Min Chang, Ashok K. Batra, and Ravindra B. Lal; *Crystal Growth and Design.*, 2002; 2: 431.
29. S. Kodie; *Phil. Mag.*, 1959; 4: 243.
30. R.V.S.S.N. Ravikumar, A. V. Chandrasekhar, B. J. Reddy, Y. P. Reddy and Jun Yamauchi; *Ferroelectrics.*, 2002; 274: 127.
31. Andreea Stanila, Cornelia Braicu, Sorin Stanila and Raluca M. Pop; *Notulae Botanicae HortiAgrobotanici.*, 2011; 39: 124.
32. J. Donohue, L.R. Lavine and J.S. Rollett; *Acta Crystallogr.*, 1956; 9: 655.
33. C.M.R. Remedios, W. Paraguassu, J. A. Lima Jr, P.T.C. Freire, J Mendes-Filho, FEA Melo, A S de Menezes, A O dos Santos, L P Cardoso and M A R Miranda; *J. Phys. Cond. Matter.*, 2008; 20: 6.

34. C. Alosious Gonsago, Helen Merina Albert, R. Umamaheswari and A. Joseph Arul Pragasam; *J Therm. Anal. Calorim.*, 2012; 110: 839.
35. S.S. Hussaini, K. Datta, P. Ghosh, S.B. Kadam and M.D. Shirsat ; *International Conf. on Opt. Phot.*, Chandigarh, India, 2009.
36. K.D. Parikh, D. J. Dave, B.B Parekh and M.J Joshi; *Cryst. Res. & Technol.*, 2010; 10: 603.
37. V. Renuga; *Int.J.Adv.Res.*, 2014; 2: 1159.
38. A. Abragam and B. Bleaney, *Electron Paramagnetic Resonance of Transition Ions*, Clarendon Press, Oxford, UK, 1970.
39. R.V.S.S.N. Ravi Kumar, A.V. Chandrasekhar, B.J Reddy, Y.P Reddy and J. Yamauchi; *Ferroelectrics.*, 2002; 274: 127.
40. F. Gan and H. Liu; *J. Non. Cryst. Solids.*, 1982; 52: 43.
41. Ch. Ramakrishna, U.S. Udaychandran Thampy, Y.P Reddy, P.S. Rao; Jun Yamauchi and R.V.S.S.N Ravikumar; *Solid State Comon.*, 2010; 150: 1479.
42. C. Shiyamala, R. Venkatesan and P. Sambasiva Rao; *J. Phys. Chem. Solids*, 2003; 64: 2329.
43. J.R. Pilbrow; *Transition Ion Electron Paramagnetic Resonance*, Clarendon Press, Oxford, UK., 1990; 148.
44. B. Sreedhar, C.Sumalatha, H. Yamada and K. Kojima; *J. Non-Cryst. Solids.*, 1996; 203: 172.
45. R.V.S.S.N Ravikumar, A.V. Chandrasekhar, L. Ramamoorthy, B.J. Reddy, Y.P. Reddy, J. Yamauchi and P.S. Rao; *J. Alloys Compd.*, 2004; 364: 176.
46. R.V.S.S.N Ravikumar, K. Ikeda, A.V. Chandrasekhar, Y.P. Reddy, J. Yamauchi and P.S. Rao; *J. Phys. Chem. Solids.*, 2003; 64: 2433.
47. W. Low; *Phys,Rev.*, 1958; 109: 256.
48. C. Alosious Gonsago, Helen Merina Albert, R. Umamaheswari and A. Joseph Arul Pragasam; *J Therm. Anal. Calorim.*, 2012; 110: 839.
49. S. Kodie; *Phil. Mag.*, 1959; 4: 243.
50. B. Natarajan, S. Mithira and P. Sambasiva Rao; *Phys. Scr.*, 2011; 83: 8.
51. R.V.S.S.N. Ravikumar, A. V. Chandrasekhar, B. J. Reddy, Y. P. Reddy and Jun Yamauchi; *Ferroelectrics.*, 2002; 274: 127.
52. Juan A. Cuadrado, Weixing Zhang, Wei Hang and Vahid Majidi; *J. Environ. Monit.*, 2000; 2: 355.
53. C.C. McDonald and W. D. Phillips; *J. Am. Chem. Soc.*, 1963; 85: 3736.

54. Lukas Gala, Michael Lawson, Klaudia Jomova, Lubomir Zelenicky, Andrea Congradyova Milan Mazur and Marian Valko; *Molecules.*, 2014; 19: 980.
55. C. Alosious Gonsago, Helen Merina Albert, R. Umamaheswari and A. Joseph Arul Pragasam; *Ind. J. Sci.Tech.*, 2012; 5: 2369.
56. C. Alosious Gonsago, Helen Merina Albert, P. Malliga and A. Joseph Arul Pragasam; *Mater. Man.Proc.*, 2012; 27: 355.
57. B. W. Mott; *Micro indentation Hardness Testing*, Butter worths, Scientific publication, London., 1956.
58. P. Anandan, G. Parthipan, T. Saravanan, R. Mohan Kumar, G. Bhagavannarayana and R. Jayavel; *Physica B: Cond. Matter.*, 2010; 405: 4951.
59. S.K. Kurtz and T.T. Perry; *J. Appl. Phys.*, 1968; 39: 3798.
60. Lyudmila Boyanova, Galina, Gergova, Rossen Nikolov, Sirigan Derejian, Elena Lazarova, Nikolai Katsarov, Ivan Mitov and Zacharii Krastev; *J. Med. Microbiol.*, 2005; 54: 481.